Nucleocytoplasmic Distribution of Opioid Growth Factor and Its Receptor in Tongue Epithelium

IAN S. ZAGON,* TORRE B. RUTH, AND PATRICIA J. MCLAUGHLIN
Department of Neural and Behavioral Sciences, Pennsylvania State University, College of Medicine, Hershey, Pennsylvania

ABSTRACT

The subcellular distributions of the opioid growth factor (OGF), [Met^5]-enkephalin, and opioid growth factor receptor (OGFr) in the epithelium of the rat tongue were determined in order to reveal structure-function relationships. Laser scanning confocal microscopic analysis showed that both OGF and OGFr were colocalized in the paranuclear cytoplasm and in the nuclei of keratinocytes in the stratum basale. Using immunoelectron microscopy and postembedding techniques, double labeling experiments disclosed that complexes of OGF-OGFr were colocalized on the outer nuclear envelope, in the paranuclear cytoplasm, perpendicular to the nuclear envelope in a putative nuclear pore complex, and in the nucleus adjacent to heterochromatin. Anti-OGF IgG alone was detected in the cytoplasm, and anti-OGFr IgG alone was associated with the outer nuclear envelope. Study of chronic treatment with the opioid antagonist, naltrexone (NTX), which blocks opioid-receptor binding, revealed the presence of OGFr immunoreactivity alone in the cytoplasm and the nucleus; some OGF-OGFr complexes were also observed. Colocalization of OGFr and karyopherin (importin) β was recorded in the cytoplasm and nucleus. These results in tongue epithelium are the first to suggest that OGFr resides on the outer nuclear envelope, where OGF interacts with OGFr; that the OGF-OGFr complex translocates between cytoplasm and nucleus at the nuclear pore; and that the nuclear localization signal of OGFr interacts with karyopherin β for nuclear transport. These novel data also indicate that signal transduction for cell proliferation appears to involve an OGF-OGFr complex that interfaces with chromatin in the nucleus. Moreover, the unique finding that OGFr was found in the cytoplasm and nucleus in NTX-treated specimens may suggest that NTX-OGFr complexes have the same pathway as OGF-OGFr. © 2004 Wiley-Liss, Inc.

Key words: nuclear localization signal; karyopherin; importin; nuclear import; nuclear receptor; opioid; immunoelectron microscopy; nucleocytoplasmic

The opioid growth factor, [Met^5]-enkephalin, is a constitutively expressed native opioid that interacts with the opioid growth factor (OGF) receptor (OGFr) to inhibit growth (cell number) in neoplasia, development, wound healing, and angiogenesis (Zagon et al., 2002). OGF is encoded by the preproenkephalin A gene (Noda et al., 1982). OGF is an autocrine and paracrine signal peptide that has a direct and rapid effect. Its actions are stereospecific, reversible, noncytotoxic, independent of serum, and occur at physiologically relevant concentrations (Zagon et al., 2002). OGF activity is not cell-, tissue-, or organ-specific and is targeted to the G0/G1 phase of the cell cycle (Zagon et al., 2002). Interruption of peptide-receptor interaction by sustained opioid receptor antagonism [e.g., naltrexone (NTX), the potent and long-acting antagonist], OGF-specific antibodies, or antisense OGFr oligoprobes results in a substantial increase in cell number (Zagon et al., 2002), suggesting that OGF and OGFr are in an autocrine loop and interface in a constitutive manner.

Receptor binding analysis with radiolabeled OGF and developing, renewing, or neoplastic cells/tissues revealed specific and saturable binding, and subcellular fractionation experiments disclosed that the binding site was associated with the nuclear fraction (Zagon et al., 2002). The subcellular distribution of OGF and OGFr has been determined in rat corneal epithelium (Zagon et al., 2003) using immunoelectron microscopy. The results show that OGFr is located on the outer nuclear envelope, and OGF interacts with OGFr at that position and appears to translocate through the nuclear pore, where it associates with chromatin in the nucleus. The cDNA for OGFr has been cloned and sequenced from rats, mice, and humans (Zagon et al., 2002). The only recognizable motif is a bipartite nuclear localization signal (NLS) in all three species. The molecular and protein structure of OGFr is unlike that of the classical opioid receptors. For example, OGFr does not belong to the superfamily of G-protein-coupled receptors and lacks the putative structure of a seven transmembrane domain.

The present study was designed to address the localization and site(s) of interaction of a growth-inhibitory peptide, OGF, and its receptor, OGFr, in dividing cells of the dorsal tongue epithelium. A second question raised in these studies relates to whether the distribution of OGF and OGFr are affected by chronic opioid receptor blockade, known to interfere with OGF-OGFr interfacing and to stimulate cell replication in actively replicating cells of the tongue epithelium. A third question in this investigation is whether the NLS encoded in OGFr is involved in the transport of this receptor from the cytoplasm to the nucleus in proliferating keratinocytes of the tongue epithelium. Complementary techniques for morphological detection included laser scanning confocal microscopy and immunoelectron microscopy using a postembedding procedure (Bendayan, 1982, 2000; Varndell and Polak, 1984; Varndell et al., 1986) and antibodies specific for OGFr (Zagon and McLaughlin, 1993; Zagon et al., 1995, 2003). These techniques not only offered structural assessment of events related to biological processes, but could also provide knowledge of the spatial organization in order to formulate a more complete picture of the mechanism and function of peptide-receptor action. Finally, the tissue chosen to perform these experiments was the stratum basale of the dorsal tongue epithelium, an easily accessible population of proliferating cells known to be regulated by OGF-OGFr interaction (Zagon et al., 1994a, 1994b). Previous investigations (Zagon et al., 1994b) of the epithelium of the rat tongue have demonstrated the presence of OGF and OGFr in the cells of the stratum basale using immunohistochemistry, and that the OGF-OGFr axis modulates DNA synthesis of these keratinocytes in a circadian rhythm-dependent manner. An understanding of the location and distribution of OGF-OGFr in normal epithelium of the tongue is important in comprehending the mechanism(s) of growth regulation of this epithelium during homeostasis. Finally, squamous cell carcinoma of the oral cavity (SCCHN) contains both OGF and OGFr, OGF modulates the growth of these cancers both in vitro and in vivo, and there is evidence that the biology and function of this peptide and receptor may be compromised in SCCHN (Levin et al., 1997; McLaughlin et al., 1999, 2003a, 2003b). Therefore, comprehension of the OGF-OGFr axis in normal epithelium will be vital to deciphering irregularities of this system in neoplastic epithelium.

MATERIALS AND METHODS

Animals

Adult (250–300 g) male Sprague-Dawley rats (Charles River Labs, Wilmington, MA) were utilized in these studies. Animals were housed in an environment of $21 \pm 0.5°C$ with a relative humidity of $50\% \pm 10\%$. The room had a complete exchange of air 15–18 times/hr and a 12-hr light-dark cycle with no twilight. Water and Purina 5010 Rodent chow were continuously available. The rats were acclimated to the animal facilities for at least 1 week prior to study.

All investigations conformed to the regulations of the National Institutes of Health and the guidelines of the Department of Comparative Medicine of the Pennsylvania State University College of Medicine. Procedures for animal utilization were approved by the Institutional Animal Care and Use Committee.

Immunohistochemistry

Immunohistochemical studies were performed to ascertain the distribution of OGF and OGFr in the tongue epithelium. The procedures outlined previously (Zagon et al., 1994b) were utilized. Three animals were anesthetized with 30 mg/kg sodium pentobarbital (intraperitoneal injection) and sacrificed by decapitation, and the entire tongue was removed immediately. In brief, specimens were rinsed in 0.1 M Sorenson's phosphate buffer (SPB; pH 7.4), frozen in isopentane chilled on dry ice, and embedded in OCT medium. Cryostat sections (15 μm) were collected on gelatin-coated slides and stored at −20°C for no longer than 14 days until processing. Tissues were fixed and permeabilized in ice-cold 100% ethanol and acetone for 10 min each, rinsed with SPB, blocked with 3% normal goat serum (NGS) in 50 mM SPB, pH 7.4. Sections were incubated in a humidified chamber at 4°C for 16–18 hr with primary antibodies to either OGF [i.e., rabbit polyclonal anti-OGF CO172 (Zagon et al., 1995), BO654 (Zagon et al., 2003)], native OGFr AO440 (Zagon and McLaughlin, 1993), or fusion protein-generated OGFr antigen 14E (IO028) (Zagon et al., 1999) that have been well characterized. Antibodies were diluted 1:150 with 1% NGS and 0.1% Triton X-100 in SPB. In some cases, sections were double-stained with a rabbit polyclonal antibody to OGF (CO172) and a chicken polyclonal antibody to OGFr (C17) generated to a recombinant OGFr protein (Cocalico Biologicals, Reamstown, PA) and characterized in Zagon et al. (2003). Secondary antibodies (Alexa Fluor) conjugated to fluorescein and rhodamine, appropriate for the primary antibody, were obtained from Molecular Probes (Eugene, OR). Sections were mounted in 60% glycerol-40% SPB and observed using an Olympus BH-2 microscope equipped with fluorescent, bright-field, and phase optics, a Zeiss LSM210 Confocal Microscope equipped with an argon and an HE/NE laser and a 63 × oil immersion PlanAchromat objective, or a Leica TCS SSP2 AOBS Confocal Microscope equipped with argon, HE/NE, and 405 Diode lasers and a 63 × oil immersion PlanAchromat objective. Sections that served as controls were incubated with secondary antibodies only or with primary antibodies preabsorbed with either an excess of OGF, the 17 kDa subunit of OGFr, or OGFr fusion protein.

At least five sections/animal were stained and examined with every antibody and for double-staining with OGF and

OGFr. Three sections/animal were studied for each of the preabsorbed and secondary antibody controls.

Electronic images from the confocal microscopy were processed using Adobe Photoshop 7.0 (Adobe Systems, San Jose, CA). The Optimas program (Optimas, Bothell, WA) was used for digital interpretation and analysis. Ten separate cells were evaluated for densitometric measurements.

Standard Electron Microscopy

For orientation and location of tissue and cell structure using our immunoelectron microscopic techniques, which necessitated less than optimal fixation techniques and a reduction in quality of the specimens, some tissues were prepared for standard electron microscopic examination. Dorsal tongue epithelium of three rats was fixed by immersion in 4% paraformaldehyde and 5% glutaraldehyde in 0.1 M cacodylate buffer containing 0.025% $CaCl_2$ for 3 hr at room temperature and a pH of 7.2. Following extensive washing, tissues were postfixed in a solution of 1% OsO_4 and 0.025% $CaCl_2$ and 0.1 M cacodylate buffer for 1 hr at room temperature and embedded in Epon 812. Semithin sections (0.5–1 μm) were prepared and stained with toluidine blue and observed with bright-field microscopy. Ultrathin sections were examined with a Philips 400 transmission electron microscope after staining with 2% uranyl acetate (1 hr) and 0.4% lead citrate (8 min). At least two blocks of tissue/animal, three grids per block, were examined with standard electron microscopy.

Immunoelectron Microscopy

Drug treatment. Some rats received twice daily injections of the opioid antagonist, NTX (30 mg/kg; > 99% purity; Sigma, St. Louis, MO) or sterile saline for 7 days. This dosage of NTX is known to invoke a continuous opioid receptor blockade in the rat (Zagon and McLaughlin, 1984) and to increase DNA synthesis in the keratinocytes of the stratum basale of the dorsal tongue epithelium in rodents (Zagon et al., 1994a).

Tissue preparation. Animals were anesthetized with 30 mg/kg sodium pentobarbital (intraperitoneal injection) and sacrificed by decapitation. The entire tongue was removed immediately, and cores of dorsal epithelium from the anterior two-thirds of the dorsal tongue were obtained using a 3 mm Acu-Punch biopsy tool (Acuderm, Ft. Lauderdale, FL). At least three cores were removed and examined from each tongue, and tissues from at least three animals/treatment group (i.e., control, NTX) were studied. The ventral surface was removed from each core, leaving the dorsal epithelium and underlying connective tissues.

Preliminary studies used a preembedding technique for immunoelectron microscopy, but antigenicity of the antibodies to OGF or OGFr was not compatible with obtaining immunoreactivity. Thus, a postembedding procedure was utilized. The postembedding technique for immunoelectron microscopy has been reported to limit problems with diffusion and penetration of staining as seen with preembedding protocols (Varndell and Polak, 1984; Berryman and Rodewald, 1990). To eliminate confounding variables, an etching protocol was not used. The methods for immunoelectron microscopy were adapted from Berryman and Rodewald (1990), which focused on preservation of membranes and antigenicity and avoidance of lipid extraction. This included a combination of primary fixatives that did

not interfere with staining and stabilized structures (e.g., low concentrations of glutaraldehyde, picric acid), the quenching of aldehydes with ammonium chloride treatment, omission of OsO_4 for postfixation after glutaraldehyde, postfixation with uranyl acetate and dehydration in acetone to minimize extraction of lipids, avoidance of complete dehydration, and low-temperature embedding. In addition, immunogold labeling rather than peroxidase was utilized to maximize analysis of the location of immunoreactivity (Bendayan et al., 1987). The hydrophilic resin unicryl was selected as the plastic embedding media because it provides good morphological preservation and allows for highly specific immunolocalization both at the light and the electron microscopic levels (Scala et al., 1992).

In brief, specimens were placed in a fixative containing 4% paraformaldehyde, 0.1% glutaraldehyde, and 0.2% picric acid in 0.1 M Sorenson's phosphate buffer with 0.5 mM $CaCl_2$ (pH 7.4) at room temperature for 3 hr. Specimens were washed in a buffer containing 0.1 M Sorenson's phosphate buffer with 3.5% sucrose and 0.5 mM $CaCl_2$ for 12 hr. Free aldehydes were quenched in 50 mM ammonium chloride in the wash buffer for 1 hr on ice. Phosphate ions were removed in a 0.1 M maleate buffer with 3.5% sucrose (pH 6.5). Tissues were postfixed in 2% uranyl acetate in ice-cold maleate buffer containing sucrose for 2 hr (pH 6.0) and dehydrated for 45 min each in 50% (4°C), 70% (−20°C), and 90% (−20°C) acetone. Samples were infiltrated sequentially for 30 min each in 3:1 acetone: unicryl, 1:1 acetone:unicryl, and 1:3 acetone:unicryl, plus two changes of 45 min each in 100% unicryl, and left overnight in 100% unicryl at −20°C. Tissues were polymerized for 3 days at 60°C. Unicryl was purchased from Vector Laboratories (Burlingame, CA).

Thin sections were collected on standard square 200-mesh nickel grids (EM Sciences, Ft. Washington, PA). The labeling procedure was performed by positioning grids on 30 μl droplets of all solutions that were placed on the surface of a sheet of Parafilm. Primary antibodies were incubated for 1 hr on a magnetic stir plate at room temperature.

Primary antibodies included well-characterized rabbit polyclonal antibodies to OGF (CO172, BO654), native OGFr (AO440), or fusion protein-generated OGFr antigen (IO028) at dilutions of 1:500 (Zagon and McLaughlin, 1993; Zagon et al., 1999, 2003). In addition, a monoclonal antibody to karyopherin (importin) β obtained from BD Biosciences (San Diego, CA) was utilized at a dilution of 1:1,000. Initial experiments were performed with AE1/AE3 anticytokeratin monoclonal antibody (1:200 dilution; Boehringer Mannheim, Indianapolis, IN) in order to establish and verify our immunoelectron microscopic protocol. Secondary antibodies with either 6 or 10 nm colloidal-gold-conjugated goat antirabbit IgG (H&L; EM Sciences) were utilized for OGF and OGFr; the secondary antibody for the monoclonal antibody was either 10 or 20 nm colloidal gold particle-conjugated to a goat antimouse IgG (EM Sciences). Secondary antibody incubation was 1 hr at room temperature.

In some cases, colocalization was conducted using the on-grid double-face immunogold labeling technique that has proven especially useful in studies that stain with antibodies produced in the same animal (Bendayan, 1982, 2000; Varndell and Polak, 1984; Varndell et al., 1986; Scala et al., 1992). This method relies on the fact that only

the antigenic sites exposed by the cutting procedures can be detected. Staining of one side of the grid is used with a primary antibody followed by incubation with a secondary antibody conjugated to a large-size gold particle. Staining of the other side of the grid is then performed with a different primary antibody and followed by processing with a secondary antibody conjugated to a small gold particle.

After each immunolabeling, sections were fixed in a 1% glutaraldehyde solution in Tris-buffered saline. Controls included specimens incubated with secondary antibodies only, or with primary antibodies preabsorbed with either an excess of OGF for the antibody to OGF, the 17 kDa binding fragment of OGFr for the antibody to native OGFr, or full-length OGFr fusion protein for the fusion protein-generated OGFr antibody.

Poststaining procedures utilized 2% uranyl acetate (20 min) and 0.4% lead citrate (10 min) solutions. Some sections were examined without poststaining. Sections were examined with a Philips 400 electron microscope. Background labeling was negligible, and positive reaction was assessed as an aggregate of two or more gold particles.

The studies focused on the keratinocytes of the stratum basale of the dorsal epithelium of the tongue because this is known to be an active area of cell proliferation in the basal cell layers (Cameron, 1966; Hume and Potten, 1983) and is regulated under homeostatic conditions by the OGF-OGFr system (Zagon et al., 1994a, 1994b).

At least eight grids/core of tissue for single (OGF, OGFr, karyopherin β, AE1/AE3) or double labeling (OGF and OGFr, OGFr and karyopherin β), and at least eight grids/core of tissue for controls (preabsorbed with the appropriate antigen, secondary antibody only), were utilized. A negative control (preabsorbed and/or secondary antibody only) was included with every staining procedure. The magnification for visualizing 20 nm immunogold (i.e., AE1/AE3) required a magnification of 16,500 ×, and observations for 6 and 10 nm colloidal gold (OGF, OGFr, karyopherin β) necessitated a magnification of at least 35,500 ×. Photomicrographs of immunogold preparations were often printed at a low contrast in order to optimize detection of the immunogold particles.

RESULTS
Light Microscopic Immunohistochemistry

Analysis of immunohistochemical preparations of the rat tongue stained with anti-OGFr IgG or anti-OGF IgG consistently revealed a strong reaction product associated with the keratinocytes of the stratum basale. Histological, electron microscopic, and immunohistochemical orientation are shown in Figures 1 and 2. OGFr and OGF were localized intracellularly and stained the paranuclear cytoplasm of cells in the stratum basale (Fig. 2B and D). Inspection of these samples also showed immunoreactivity as a speckling pattern within the nucleus (Fig. 2B, D, and F). OGF and OGFr were found to be colocalized in both the cytoplasm and nucleus of keratinocytes of the stratum basale as demonstrated visually (Fig. 2A and F) and by image analysis (see histogram, Fig. 2). Staining with antibodies to OGF or OGFr that were preabsorbed with respective antigens (Fig. 2C and E), and those processed with the secondary antibody only (data not shown), consistently showed negligible immunoreaction.

Immunoelectron Microscopy: Methodological Considerations

A protocol for staining of sections with antibodies to OGF and OGFr for immunoelectron microscopy was developed, with the final procedure given above. Some highlights of our preliminary findings include the use of a preembedding rather than postembedding technique and initial studies performed with a polyclonal antibody to AE1/AE3 in order to verify the immunoelectron microscopic staining procedure. Following the report of Mount and Taatjes (1994), immunoreactivity to AE1/AE3 was associated with the cytokeratin bundles in the tongue (data not shown). A range (0.1–2%) of glutaraldehyde concentrations were explored, and the highest concentration compatible with antigenicity for OGF or OGFr was determined (i.e., 1% glutaraldehyde). Dehydration in acetone, rather than ethanol, incomplete dehydration to a 90% acetone solution, and the elimination of propylene oxide optimized antigenicity. Although a variety of embedding media was explored (e.g., Lowicryl, Epon 812), unicryl, a low-molecular-weight hydrophilic resin, minimized the loss of antigenicity and possessed excellent infiltration properties.

Immunoelectron Microscopic Location of OGFr

Immunogold related to OGFr was localized to the cells in the stratum basale of the dorsal tongue epithelium in electron microscopic preparations (Figs. 3, 5, 6, and 7); no differences in OGFr deposition were found between sections. Label for anti-OGFr IgG could be discerned in association with the outer nuclear envelope (Figs. 3A, 5A, and 6B). Groupings of immunogold related to OGFr were located in regions of the cytoplasm that extended to no more than 0.5 μm from the nuclear envelope and were considered to be in the paranuclear cytoplasm (Figs. 3B, 5B, 6B, and 7A). Anti-OGFr IgG was recorded spanning between the outer and inner nuclear membranes and localized in the perinuclear space, and immunogold was arranged in a perpendicular position to the nuclear envelope (Figs. 3C, 5C, and 7B). Although precise identification was compromised because of the limitations in fixation (e.g., low glutaraldehyde concentration and omission of postfixation with osmium tetroxide needed for antigenicity), this OGFr immunoreactivity was believed to be associated with a putative nuclear pore complex (NPC; Figs. 3C, 5C, and 7B). In the nucleus, immunoreactivity related to OGFr could be observed in relationship to heterochromatin aggregations (Figs. 3D, 5D, 6A, and 7C) and, in some instances, proximal to the inner nuclear lamina (Figs. 3D, 5D, and 6A). Preabsorbed control preparations and those stained with the secondary antibody showed little immunoreactivity in keratinocytes of the stratum basale (Fig. 3E).

Immunoelectron Microscopic Location of OGF

Immunostaining of OGF (Figs. 4–6) showed a distribution in the cells of the stratum basale often resembling that seen with OGFr (Figs. 3, 5, 6, and 7); the deposition of OGF in all sections was similar. Immunogold related to OGF was deposited on the outer nuclear envelope (Figs. 4C, 5A, and 6B), in a paranuclear position (Figs. 4B and 5B), perpendicular to the nuclear envelope at a putative NPC (Figs. 4D and 5C), and in association with electron-dense chromatin (Figs. 4E and 5D). In addition, aggre-
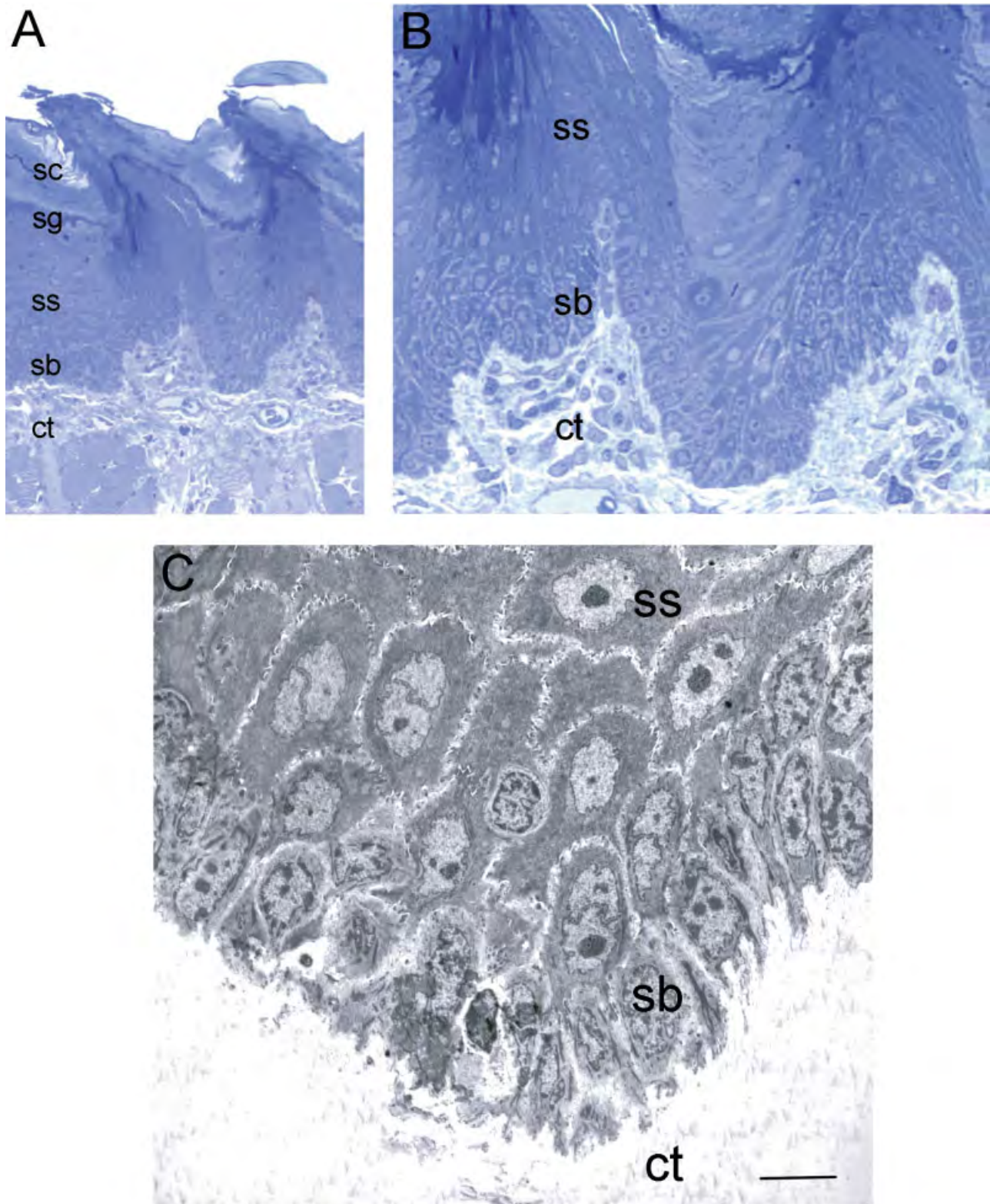
Fig. 1. Low-power (**A**) and higher-power (**B**) bright-field photomicrographs of semithin sections and a low-magnification electron micrograph (**C**) of the dorsal epithelium of rat tongue. Immunoelectron microscopic studies focused on the keratinocytes of the stratum basale of epithelium. sb, stratum basale; ss, stratum spinosum; sg, stratum granulosum; sc, stratum corneum; ct, connective tissue. Scale bar = 80 μm (A), 35 μm (B), and 6 μm (C).
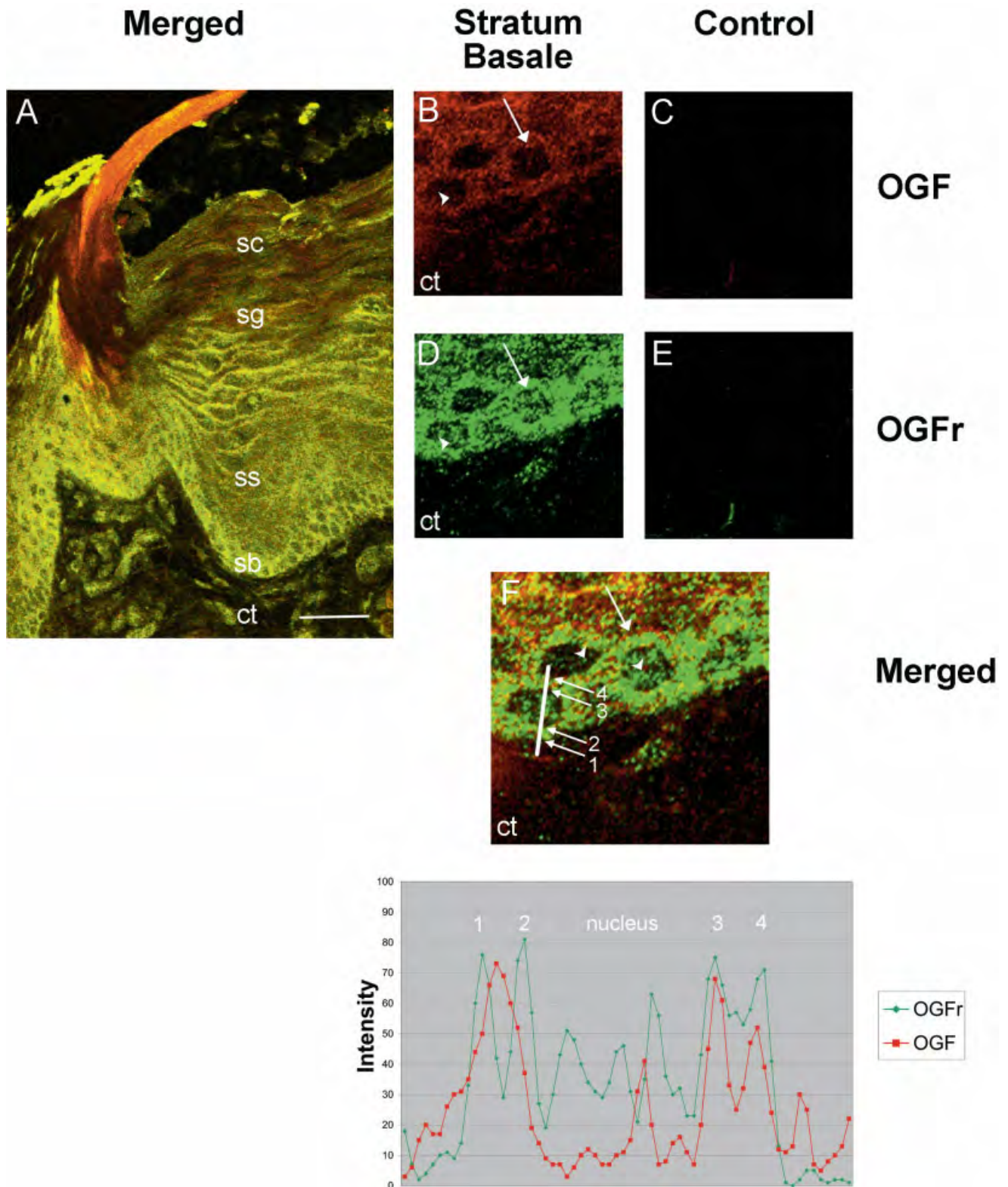
Fig. 2. Confocal images of immunohistochemical preparations of the dorsal epithelium of the adult rat tongue stained with antibodies to OGFr, OGF, or both OGFr and OGF and examined by confocal laser scanning microscopy. **A:** A merged low-power micrograph of a specimen stained with both OGF and OGFr providing orientation for location of the stratum basale in B–F. Note the intense staining of the cytoplasm of keratinocytes of the stratum basale. Cells of the stratum basale of the tongue epithelium stained with antibodies to OGF (**B** and **C**) or OGFr (**D** and **E**); preparations in C and E are preabsorbed with OGF (C) or OGFr (E). Staining of the perinuclear cytoplasm (arrows) and a speckling pattern of immunoreactivity within nuclei (arrowheads) in the keratinocytes of the stratum basale (B and D) were observed. **F:** A merged image of the specimen in B and D stained with OGF and OGFr, respectively. Staining of the perinuclear cytoplasm (arrows) and immunoreactivity in nuclei (arrowheads) are noted. A histogram of the densitometric analyses of intensity through a keratinocyte of the stratum basale is presented beneath the merged immunohistochemical preparation demonstrating the colocalization of OGFr and OGF. Location of signal recorded in F is denoted by a solid white line; 1 and 4, proximal to plasma membrane; 2 and 3, proximal to nuclear envelope. sb, stratum basale; ss, stratum spinosum; sg, stratum granulosum; sc, stratum corneum; ct, connective tissue. Scale bar = 60 μm (A), 12 μm (B–E), and 8 μm (F).
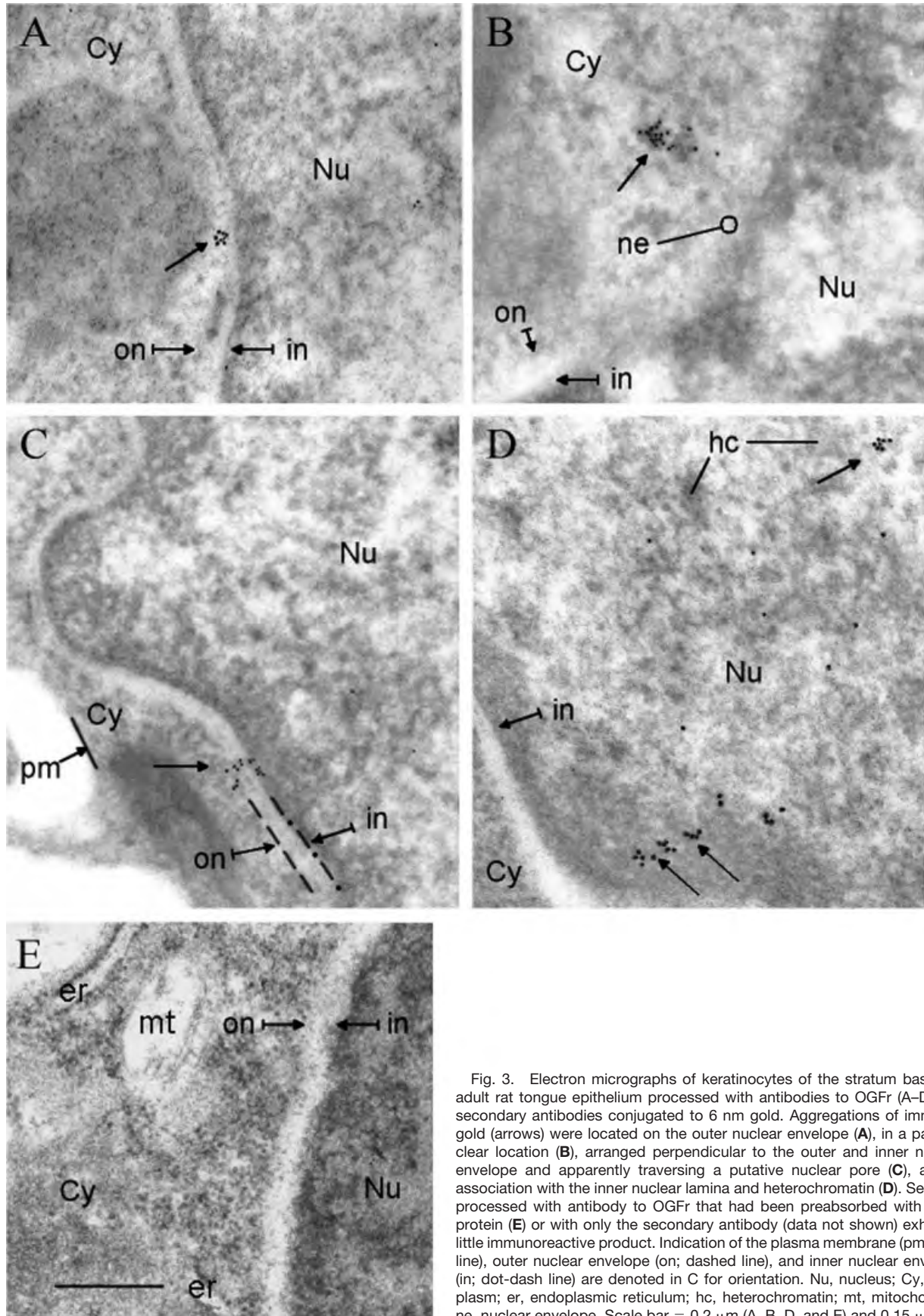
Fig. 3. Electron micrographs of keratinocytes of the stratum basale in adult rat tongue epithelium processed with antibodies to OGFr (A–D) and secondary antibodies conjugated to 6 nm gold. Aggregations of immunogold (arrows) were located on the outer nuclear envelope (**A**), in a paranuclear location (**B**), arranged perpendicular to the outer and inner nuclear envelope and apparently traversing a putative nuclear pore (**C**), and in association with the inner nuclear lamina and heterochromatin (**D**). Sections processed with antibody to OGFr that had been preabsorbed with OGFr protein (**E**) or with only the secondary antibody (data not shown) exhibited little immunoreactive product. Indication of the plasma membrane (pm; solid line), outer nuclear envelope (on; dashed line), and inner nuclear envelope (in; dot-dash line) are denoted in C for orientation. Nu, nucleus; Cy, cytoplasm; er, endoplasmic reticulum; hc, heterochromatin; mt, mitochondria; ne, nuclear envelope. Scale bar = 0.2 μm (A, B, D, and E) and 0.15 μm (C).

gates of immunogold for OGF were distributed throughout the cytoplasm and beyond the paranuclear location (more than 0.5 μm from the nuclear envelope; Figs. 4A, 5B, and 6A). Indeed, OGF immunostaining could be seen even proximal to the plasma membrane (Fig. 4A) of keratinocytes of the stratum basale. Preabsorbed control preparations and those stained with the secondary antibody showed little immunoreactivity (Fig. 4F) in cells of the stratum basale.

Immunoelectron Microscopic Colocalization of OGFr and OGF

Although single labeling of OGFr (Fig. 3) and of OGF (Fig. 4) were often distributed to the same cellular regions as recorded by immunoelectron microscopy, and colocalization studies with confocal microscopy indicated overlap (Fig. 2), whether these molecules were localized to the same site required elucidation. Using immunoelectron microscopy and double-face labeling technique (Varndell and Polak, 1984; Varndell et al., 1984; Bendayan, 2000; Zagon et al., 2003) in order to study localization of two polyclonal antibodies made in the same species, immunogold for both OGFr and OGF were detected adjacent to the outer nuclear envelope (Fig. 5A and 6B), in the paranuclear cytoplasm (Fig. 5B), perpendicular to the nuclear envelope in the perinuclear space (Fig. 5C), and in association with the inner nuclear matrix and at the border of heterochromatin (Fig. 5D). Anti-OGFr IgG, but not anti-OGF IgG, sometimes could be observed on the outer nuclear envelope in these dual-labeled preparations (data not shown). Complexes of OGF and OGFr were not detected in the cytoplasm extending beyond the paranuclear location. However, unbound OGF immunogold, but not OGFr, was seen in the peripheral cytoplasm and occasionally proximal to the plasma membrane. (Fig. 6A). The observations of colocalization of OGF and OGFr were comparable in all the sections examined.

Opioid Receptor Blockade and OGF-OGFr Distribution

Persistent interruption of OGF-OGFr interfacing using opioid antagonists such as NTX is known to increase DNA synthesis (Zagon et al., 1994a). Our expectation was that NTX interacts with OGFr and remains at the site (i.e., outer nuclear envelope) of this interfacing. To investigate this thesis, the ramifications of receptor blockade with respect to the disposition of OGFr and OGF, specimens chronically exposed to NTX for 7 days, were processed for double labeling immunoelectron microscopy with OGFr and OGF (Fig. 6). Antibodies to NTX were not available to perform single label or double label (e.g., NTX and OGFr) studies directly. In double-labeled preparations of the tongue from NTX-treated rats, immunoreactive OGFr alone was found on the outer nuclear envelope, in the paranuclear location, and perpendicular to the nuclear envelope, as well as at the heterochromatin-euchromatin border (Fig. 6A). OGF immunoreactivity alone was detected in the cytoplasm of these NTX-exposed specimens that were double-labeled with antibodies to OGF and OGFr (Fig. 6A). However, on occasion (e.g., an average of one observation per section), colocalization of OGFr and OGF in the keratinocytes of the stratum basale of the tongue epithelium of animals receiving chronic NTX treatment was observed at the outer nuclear envelope (Fig. 6B),

paranuclear cytoplasm, at putative NPC, and in the nucleus. No differences between sections could be recorded as to the location of OGF and OGFr in keratinocytes from dorsal tongue of animals treated with NTX.

Karyopherin β and OGFr Localization

An NLS has been found for OGFr cDNA in the rat, mouse, and human (Zagon et al., 2002); in fact, there are 2 NLS contained in the rat and mouse OGFr cDNA (Zagon et al., 2002). Given the literature showing involvement of the NLS with karyopherin β (Gorlich and Kutay, 1999; Gasiorowski and Dean, 2003), further information was sought about the interaction of the OGFr and transport of the OGF-OGFr complex from the cytoplasm to the nucleus. Using an antibody to karyopherin β and an antibody to OGFr, double labeling studies were conducted (Fig. 7). Although karyopherin β and OGFr were found alone in the cytoplasm and the nucleus, colocalization of karyopherin β and OGFr was observed in the paranuclear cytoplasm (Fig. 7A), perpendicular to the nuclear envelope in the perinuclear space (Fig. 7B), and in the nucleus (Fig. 7C). The distribution of OGFr and karyopherin β in all sections was comparable.

DISCUSSION

Using techniques of confocal and immunoelectron microscopy, this is the first report about the subcellular localization of both OGF and OGFr in the epithelium of the rat tongue. The results concerning the distribution of OGF and OGFr in keratinocytes of the stratum basale of dorsal tongue epithelium extend observations described previously for this peptide and receptor in the corneal epithelium (Zagon et al., 2003). Together, these data yield a number of generalizable characteristics of OGF-OGFr interaction, and interpretation of this descriptive study may yield insight into the function and mechanism of this peptide and receptor. A summary diagram of the putative trafficking pattern of OGF and OGFr, based on the spatial relationship of peptide and receptor, using static images of light and electron micrographs is included in Figure 8. First, colocalization of OGF with OGFr at various locations in the cell suggests that the signaling of changes in cell proliferation by the OGF-OGFr axis is reliant on a complex of both the peptide and the receptor rather than a singular interaction at one site, which cascades into another pathway. Second, the OGF receptor, but not OGF, was sometimes found alone on the outer nuclear envelope, thereby implying the position of the unoccupied OGF receptor. These data also suggest the locale where OGF may initially interact with OGFr and may offer insight into the directionality of movement from the outer nuclear envelope (OGFr singularly as well as OGF-OGFr complexes) to the nucleus (only OGF-OGFr complexes). Third, the finding of OGF-OGFr complexes in the paranuclear cytoplasm may indicate the repositioning of peptide-receptor from the outer nuclear envelope to the cytoplasm and introduces the concept that the peptide and receptor remain bound to one another after dissociating from the outer nuclear envelope. Fourth, the colocalization of OGF and OGFr at putative NPC would signify the translocation from the cytoplasm to the nucleus. Evidence presented in this report and discussed later would suggest that OGFr utilizes at least in part the NLS as nuclear import machinery. Fifth, the finding of OGF-OGFr complexes in the
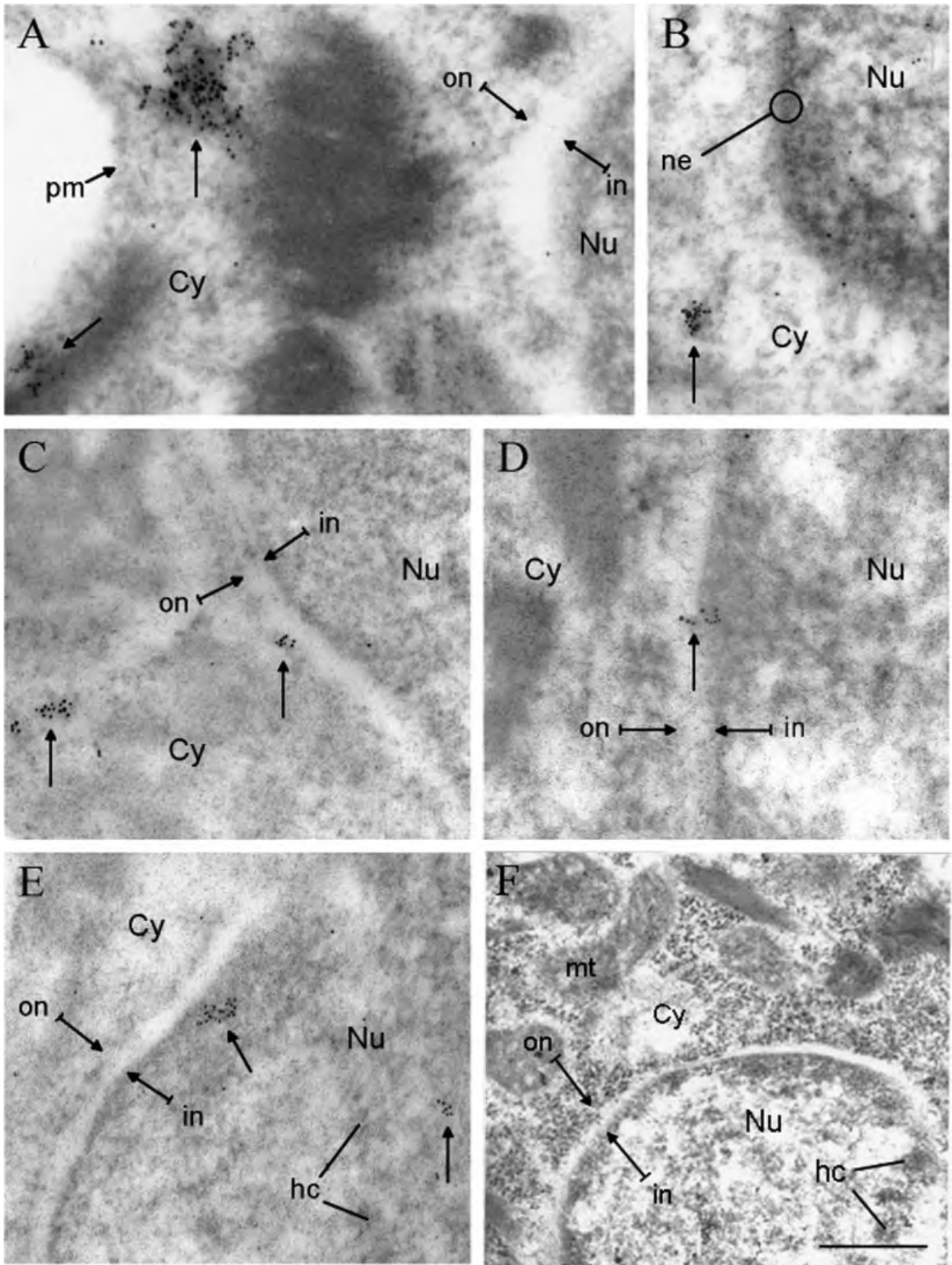
Fig. 4. Electron micrographs of keratinocytes in the stratum basale of adult rat tongue epithelium processed with antibodies to OGF (A–E) and secondary antibodies conjugated to 6 nm gold. Aggregations of 6 nm immunogold (arrows) were detected throughout the cytoplasm (A–C) and even proximal to the plasma membrane (A). Anti-OGF IgG could be found in a paranuclear position (B), in association with the outer nuclear envelope (C), extending from the outer to the inner nuclear envelope within a putative nuclear pore (D), and in close relation to both the inner nuclear lamina and the periphery of heterochromatin aggregations (E). Sections processed with antibody to OGF that had been preabsorbed with OGF (F) or with only the secondary antibody (data not shown) exhibited little immunoreactive product. Nu, nucleus; Cy, cytoplasm; hc, heterochromatin; in, inner nuclear envelope; mt, mitochondria; ne, nuclear envelope; on, outer nuclear envelope; pm, plasma membrane. Scale bar = 0.2 μm.
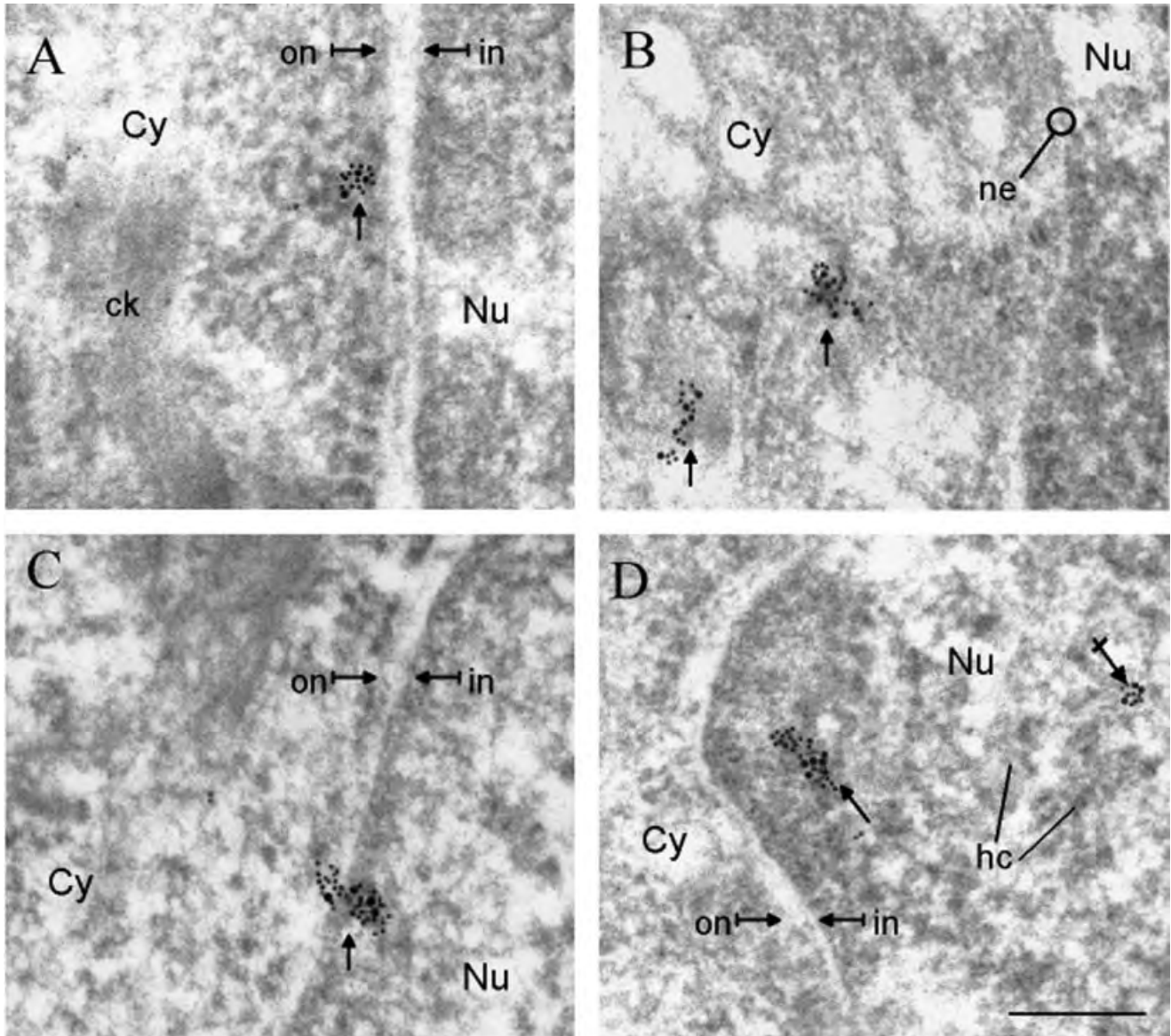
Fig. 5. Electron micrographs of keratinocytes in the stratum basale of adult rat tongue epithelium processed by dual labeling with antibodies to OGF and OGFr (A–D). OGF = 10 nm gold; OGFr = 6 nm gold. Colocalization of OGF and OGFr (arrows) on the outer nuclear envelope (**A**), paranuclear cytoplasm (**B**), extending from the cytoplasm to the nucleus in a putative nuclear pore (**C**), and associated with the inner nuclear lamina and at the periphery of heterochromatin aggregations (crosshatched arrows; **D**). Nu, nucleus; Cy, cytoplasm; hc, heterochromatin; in, inner nuclear envelope; ne, nuclear envelope; on, outer nuclear envelope; ck, cytokeratin. Scale bar = 0.2 μm.

nucleus and associated with chromatin is consistent with the ability of this axis to modulate DNA synthesis, and this function is dependent on the presence, union, and configuration of both the peptide and the receptor. Sixth, at least under homeostatic conditions, the evidence suggests there are unoccupied OGF receptors on the outer nuclear envelope of cells in the basal layer and unbound OGF in the cytoplasm of these cells. Such unoccupied receptors and free peptide would allow adaptability for the magnitude of modulation in DNA synthesis (e.g., more occupied receptors would infer a greater decrease in DNA synthesis) reported in mitotically active basal cells.

Cloning and sequencing of the OGFr revealed a motif of a bipartite NLS in the rat, mouse, and human (Robbins et al., 1991). Active nuclear import of NLS-containing proteins is mediated by the importin family of transport molecules, collectively known as karyopherins (Gorlich and Kutay, 1999; Gasiorowski et al., 2003; Xu and Massague, 2004). Proteins with an NLS are bound by karyopherin (importin) α, which acts as an adapter molecule that binds both the NLS of the cargo protein and karyopherin β (Fig. 8). Alternatively, karyopherin β can directly bind to the NLS independent of karyopherin α. α/β/NLS or β/NLS multiprotein complexes localize to the nuclear envelope as
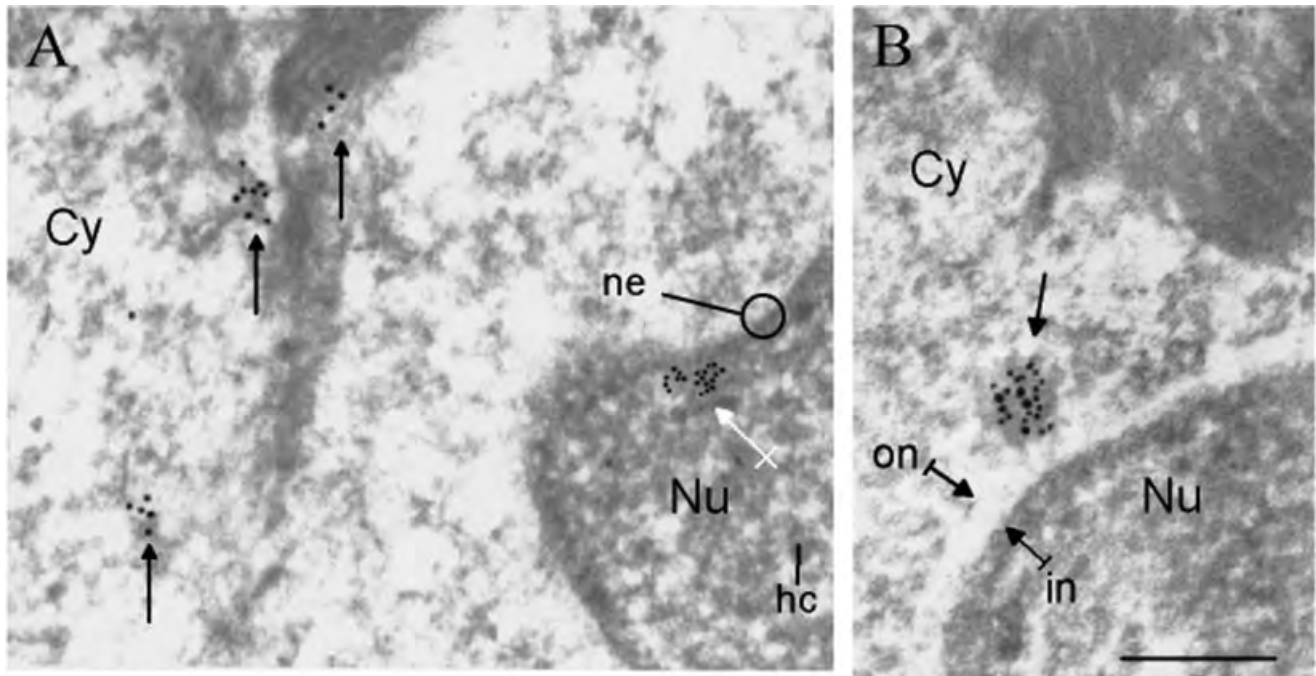
Fig. 6. Electron micrographs of keratinocytes in the stratum basale of adult rat dorsal tongue epithelium from animals treated for 7 days with twice daily injections of the opioid antagonist, NTX. Sections were processed by dual labeling with antibodies to OGFr (6 nm gold) and OGF (10 nm gold). **A:** The most frequent observation of these experiments was of OGF alone in the cytoplasm (arrows) and OGFr alone in the nucleus (cross-hatched arrow), as well as in the paranuclear region (data not shown). **B:** In some instances, OGFr could be observed to be colocalized with OGF (arrow), indicating that despite opioid receptor blockade with NTX, OGFr-OGF binding does occur. Nu, nucleus; Cy, cytoplasm; hc, heterochromatin; in, inner nuclear envelope; ne, nuclear envelope; on, outer nuclear envelope. Scale bar = 0.2 μm.

karyopherin β binds to fiber-like proteins that protrude from the nuclear pore complex into the cytoplasm, where the import substrate associates with another soluble protein, RanGDP (along with other factors such as NTF2), and subsequently is translocated through the pore. To begin to examine the transport mechanism of OGF-OGFr complexes from cytoplasm to nucleus, the present study revealed for the first time the colocalization of OGFr and karyopherin β. These data would suggest that the OGF-OGFr complex is dependent at least in part on nuclear import machinery related to the karyopherins. Further research is required to define the entire sequence of events and the proteins involved with the translocation of the OGF-OGFr complex from the cytoplasm to the nucleus.

Although the OGF receptor does not have any molecular homology to classical opioid receptors (e.g., μ, δ, κ) (Zagon et al., 2002), OGF-OGFr interactions (pharmacological, biochemical, physiological) are similar to those associated with opioid receptor mediation (e.g., naloxone-reversible, stereospecific) (Zagon et al., 2002). In the mammalian tongue epithelium, the potent and long-acting opioid receptor antagonist NTX has been reported to modulate the effects of opioid peptides on cell replicative processes, stimulating DNA synthesis in a circadian rhythm-dependent fashion (Zagon et al., 1994a). Although we hypothesized that NTX interacted with OGFr at the outer nuclear envelope and remained in this position, to our surprise, animals receiving chronic NTX treatment (known to invoke a sustained opioid receptor blockade (Zagon and McLaughlin, 1984)) were found to have OGFr immunoreactivity in the cytoplasm and nucleus. These data would suggest that NTX exposure results in a distribution of OGFr in locations similar to that found in control (normal) specimens. Whether this is free OGFr (e.g., NTX triggers the release of OGFr and it translocates to the nucleus), or OGFr is bound to NTX (i.e., NTX-OGFr complex), will require double labeling studies with OGFr and NTX; unfortunately, antibodies to NTX were not available to test this thesis. To examine whether NTX completely blocked OGF-OGFr interaction, we performed double labeling studies with OGF and OGFr. Unexpectedly, some OGF-OGFr complexes were found in cytoplasmic and nuclear locations in keratinocytes from animals with a chronic opioid receptor blockade, in a manner similar to that documented for control specimens. These intriguing results suggest that NTX may not completely block OGF-OGFr interfacing under these conditions, or that OGF-OGFr complexes represent associations of peptide and receptor that were initiated prior to NTX treatment. Given reports (Hess et al., 2003) that fluorescein-labeled NTX can traffic to the nucleus in COS cells growing in tissue culture, and that this tagged NTX is colocalized with OGFr, the present observations would be consistent with the hypothesis that OGFr in association with NTX (and not in a free form) undergoes cytoplasmic-nuclear translocation. If, on subsequent examination, this is the case, then the stimulation of cell proliferation by NTX may be due to the differences in dynamics (e.g., folding) between NTX or
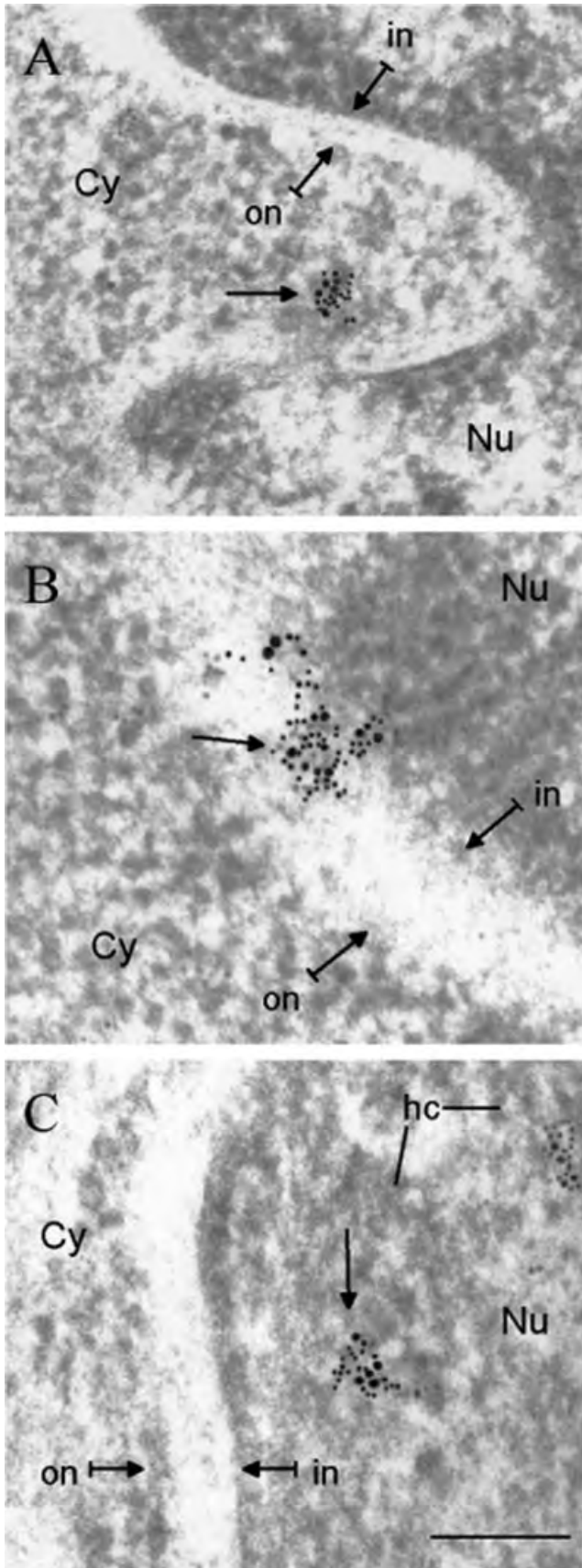
OGF with the OGF receptor when these interact with chromatin in the nucleus.

A number of methodological controls supported the data presented. A considerable number of sections were examined for single and double labeling studies, and all of the observations were consistent. This would suggest that at least given the present immunological technique, there were no discrepancies in the observations. With respect to antibody specificity, all of the antibodies have been characterized (e.g., Western blotting, quantitative immunodot assay), and preabsorbed controls along with omission of the secondary antibody were employed. Two antibodies for each antigen were used to eliminate artifacts that may be related to a particular antibody. Finally, the antibodies to OGF and to OGFr did not always localize to the same structures, indicating that there are specific characteristics and patterns of localization for each immunocytochemical reaction. However, single and double labeling studies with antibodies to a particular antigen were localized to the same anatomical substrates, providing conformation of antibody selectivity and consistency. In regard to structural biology, we used tissues fixed with conventional methods to ensure proper orientation for the less than optimal ultrastructure associated with immunoelectron microscopy. The stratification of layers in the tongue epithelium also contributed to understanding label distribution, as did the confining of the study to keratinocytes of the stratum basale, thereby circumventing regional differences. However, even though immunocytochemical localization at the ultrastructural level is a powerful technique to demonstrate relationships between cell structure and function, a central problem in immunocytochemistry is the retention of antigenicity without sacrificing cell morphology (Varndell and Polak, 1984; Bendayan et al., 1987; Berryman and Rodewald, 1990; Scala et al., 1992). The need in the present study to maintain antigenicity with the use of a low concentration of glutaraldehyde limited the preservation of structure. This raises the question of whether OGF and/or OGFr may be associated with other structures that were not preserved with the current procedures. In future studies exploring OGF and OGFr with immunoelectron microscopy, such limitation in structural detail because of methodological restrictions needs refinement (e.g., cryoimmuoelectron microscopy, alternatives to glutaraldehye, antigen retrieval) so as to reveal even greater information about peptide and receptor localization and interfacing.

ACKNOWLEDGMENTS

Fig. 7. Electron micrographs of keratinocytes in the stratum basale of adult rat dorsal tongue epithelium processed by double labeling (arrows) with antibodies to OGFr (6 nm gold) and karyopherin β (10 nm gold). Colocalization (arrows) was detected in the paranuclear cytoplasm (**A**), extending from the cytoplasm to the nucleus and traversing the perinuclear space at a putative nuclear pore (**B**), and in the nucleus (**C**). Nu, nucleus; Cy, cytoplasm; hc, heterochromatin; in, inner nuclear envelope; on, outer nuclear envelope. Scale bar = 0.2 μm.
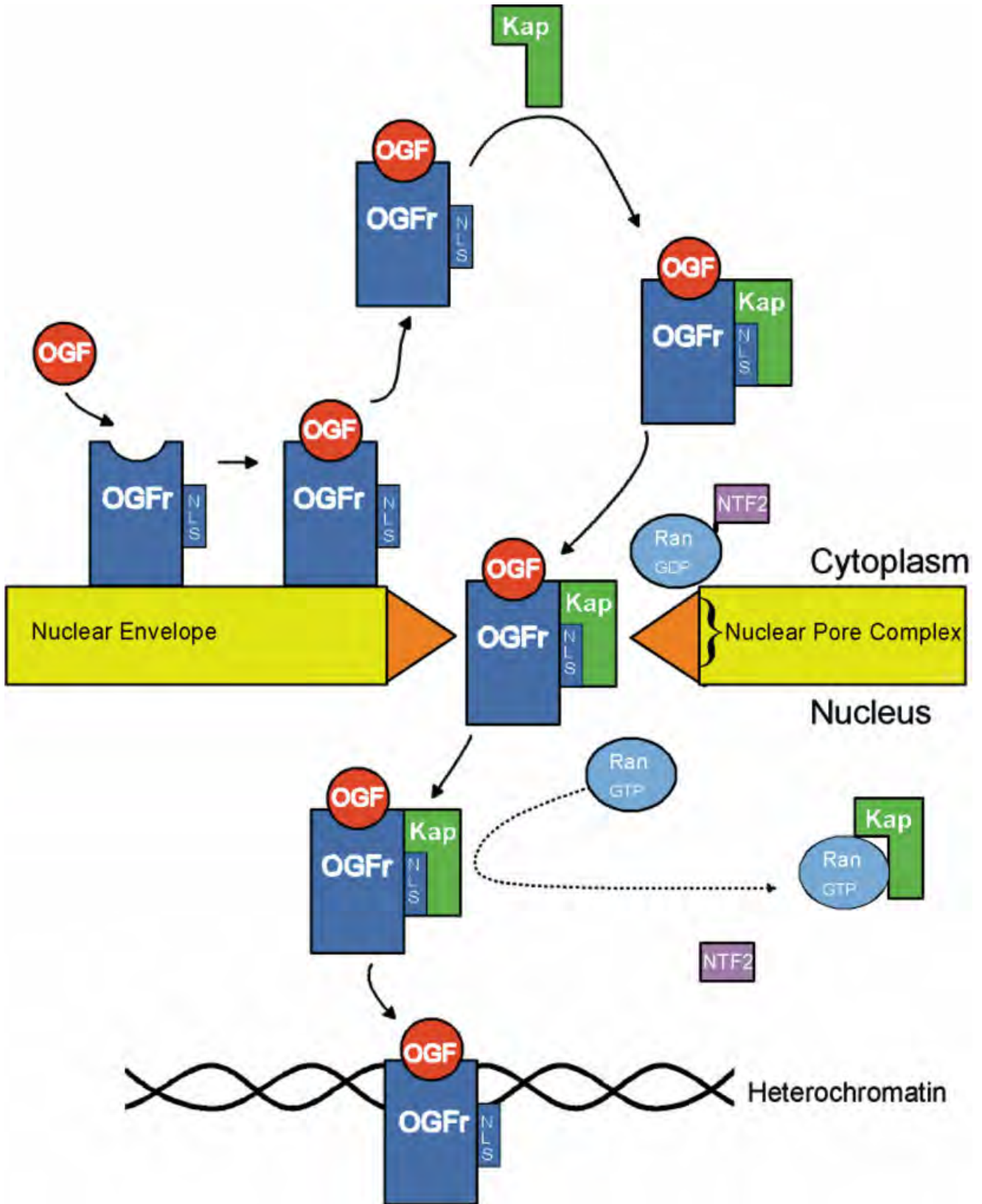
Fig. 8. Schematic of a hypothetical model of nucleocytoplasmic trafficking and interactions of OGF, OGFr, and related molecules (e.g., karyopherin β) that play a role in the tonic inhibition of DNA synthesis by the OGF-OGFr axis. The model is based on immunoelectron microscopic findings. Kap, karyopherin β; NLS, nuclear localization signal.

LITERATURE CITED

Bendayan M. 1982. Double immunocytochemistry labeling applying the protein A-gold technique. J Histochem Cytochem 30:81–85.

Bendayan M, Nanci A, Kan FWK. 1987. Effect of tissue processing on colloidal gold cytochemistry. J Histochem Cytochem 35:983–996.

Bendayan M. 2000. A review of the potential and versatility of colloidal gold cytochemical labeling for molecular morphology. Biotech Histochem 75:203–242.

Berryman MA, Rodewald RD. 1990. An enhanced method for post-embedding immunocytochemical staining which preserves cell membranes, J Histochem Cytochem 38:159–170.

Cameron IL. 1966. Cell proliferation, migration, and specialization in the epithelium of the mouse tongue. Anat Rec 184:265–274.

Gasiorowski JZ, Dean DA. 2003. Mechanisms of nuclear transport and interventions. Adv Drug Deliver Rev 55:703–716.

Gorlich D, Kutay U. 1999. Transport between the cell nucleus and the cytoplasm. Annu Rev Cell Devel Biol 15:607–660.

Hess GD, McLaughlin PJ, Zagon IS. 2003. Naltrexone trafficking in COS-7 cells. FASEB J 17:A1216.

Hume WJ, Potten CS. 1983. Proliferative units in stratified squamous epithelium. Clin Exp Dermatol 8:95–106.

Levin RJ, Wu Y, McLaughlin PJ, Zagon IS. 1997. Expression of the opioid growth factor, [Met⁵]-enkephalin, and the zeta opioid receptor in head and neck squamous cell carcinoma. Laryngoscope 107:335–339.

McLaughlin PJ, Levin RJ, Zagon IS. 1999. Regulation of human head and neck squamous cell carcinoma growth in tissue culture by opioid growth factor. Int J Oncol 14:991–998.

McLaughlin PJ, Levin RJ, Zagon IS. 2003a. Opioid growth factor (OGF) inhibits the progression of human squamous cell carcinoma of the head and neck transplanted into nude mice. Cancer Lett 199:209–217.

McLaughlin PJ, Stack BC, Levin RJ, Fedok F, Zagon IS. 2003b. Defects in the opioid growth factor receptor in human squamous cell carcinoma of the head and neck. Cancer 97:1701–1710.

Mount SL, Taatjes DJ. 1994. Neuroendocrine carcinoma of the skin (Merkel cell carcinoma): an immunoelectron-microscopic case study. Amer J Dermatopathol 16:60–65.

Noda M, Furutani Y, Takahashi H, Toosata M, Hirose T, Inayama S, Nakanishi S, Numa S. 1982. Cloning and sequence analysis of cDNA for bovine adrenal preproenkephalin. Nature 295:202–206.

Robbins J, Dilworth SM, Laskey RA, Dingwall C. 1991. Two interdependent basic domains in nucleoplasmin nuclear targeting sequence: identification of a class of bipartite nuclear targeting sequence. Cell 64:615–623.

Scala C, Cenacchi C, Ferrari C, Pasquinelli G, Preda P, Manara GC. 1992. A new acrylic resin formulation: a useful tool for histological, ultrastructural, and immunocytochemical investigations. J Histochem Cytochem 40:1799–1804.

Varndell IM, Polak JM. 1984. Immunolabelling for electron microscopy. New York: Elsevier. p 155–177.

Varndell IM, Sikri KL, Hennessy RJ, Goodman RH, Benoit R, Diani AR, Polak JM. 1986. Somatostatin-containing D cells exhibit immunoreactivity for rat somatostatin cryptic peptide in six mammalian species. Cell Tissue Res 246:197–204.

Xu L, Massague J. 2004. Nucleocytoplasmic shuttling of signal transducers. Nat Rev Mol Cell Biol 5:1–11.

Zagon IS, McLaughlin PJ. 1984. Naltrexone modulates body and brain development in rats: a role for endogenous opioid systems in growth. Life Sci 35:2057–2064.

Zagon IS, McLaughlin PJ. 1993. Production and characterization of polyclonal and monoclonal antibodies to zeta (ζ) opioid receptor. Brain Res 630:295–302.

Zagon IS, Wu Y, McLaughlin PJ. 1994a. Opioid antagonist modulation of DNA synthesis in mouse tongue epithelium is circadian dependent. Pharmacol Biochem Behav 48:709–714.

Zagon IS, Wu Y, McLaughlin PJ. 1994b. Opioid growth factor inhibits DNA synthesis in mouse tongue epithelium in a circadian rhythm-dependent manner. Am J Physiol 267:R645–R652.

Zagon IS, Sassani JW, Allison G, McLaughlin PJ. 1995. Conserved expression of the opioid growth factor, [Met⁵]-enkephalin, and the zeta (ζ) opioid receptor in vertebrate cornea. Brain Res 671:105–111.

Zagon IS, Verderame MF, Allen SS, McLaughlin PJ. 1999. Cloning, sequencing, expression and function of a cDNA encoding a receptor for the opioid growth factor, [Met⁵]-enkephalin. Brain Res 849:147–154.

Zagon IS, Verderame MF, McLaughlin PJ. 2002. The biology of the opioid growth factor receptor (OGFr). Brain Res Rev 38:351–376.

Zagon IS, Ruth TB, Leure-duPree AE, Sassani JW, McLaughlin PJ. 2003. Immunoelectron microscopic localization of the opioid growth factor receptor (OGFr) and OGF in the cornea. Brain Res 967:37–47.